Regulation of *RAD53* by the *ATM*-Like Kinases *MEC1* and *TEL1* in Yeast Cell Cycle Checkpoint Pathways

Yolanda Sanchez, Brian A. Desany, William J. Jones, Qinghua Liu, Bin Wang, Stephen J. Elledge*

Mutants of the *Saccharomyces cerevisiae* ataxia telangiectasia mutated (*ATM*) homolog *MEC1/SAD3/ESR1* were identified that could live only if the *RAD53/SAD1* checkpoint kinase was overproduced. *MEC1* and a structurally related gene, *TEL1*, have overlapping functions in response to DNA damage and replication blocks that in mutants can be provided by overproduction of *RAD53*. Both *MEC1* and *TEL1* were found to control phosphorylation of Rad53p in response to DNA damage. These results indicate that *RAD53* is a signal transducer in the DNA damage and replication checkpoint pathways and functions downstream of two members of the *ATM* lipid kinase family. Because several members of this pathway are conserved among eukaryotes, it is likely that a *RAD53*-related kinase will function downstream of the human *ATM* gene product and play an important role in the mammalian response to DNA damage.

The ability to coordinate cell cycle transitions in response to genotoxic stress is critical to the maintenance of genomic stability. Mutations in mammalian genes that abrogate this response, such as *p53* and *ATM*, cause a genetic predisposition to cancer (*1*). In yeast, several genes have been identified that control the cell cycle response to DNA damage, replication blocks, or both, including the *MEC*, *SAD*, *RAD*, and *DUN* genes. DNA polymerase ε (*POL2/DUN2*) is a potential sensor of DNA replication blocks that links the replication machinery to the S phase checkpoint (*2*). *RAD53* (also known as *SAD1*, *MEC2*, or *SPK1*) encodes a protein kinase (*3*, *4*) that controls cell cycle arrest and transcriptional responses to DNA damage and DNA replication blocks (*3*), including activation of the *DUN1* kinase (*3*, *5*). *MEC1* (also called *ESR1* or *SAD3*) encodes a protein with sequence similarity to lipid kinases that is involved in meiotic recombination (*3*) and, like *RAD53*, in the transcriptional and cell cycle responses to DNA damage and replication blocks. Mec1p belongs to the phosphatidylinositol kinase family that includes the *Schizosaccharomyces pombe rad3* checkpoint gene (*6*), *S. cerevisiae* YBL088, recently identified as *TEL1*, required for telomere maintenance (*7*), *Drosophila melanogaster mei-41* (*8*), and human *ATM* (*9*). *ATM* is mutated in patients with ataxia telangiectasia, a fatal disease characterized by autosomal recessive inheritance, immunological impairment, ataxia associated with progressive cerebellar Purkinje cell death, and a high incidence of cancer (*1*, *9*, *10*). Approximately 1% of humans are heterozygotes for *ATM* defects and show an increased incidence of cancer (*10*). *ATM*-defective cells show checkpoint defects similar to those of *mec1* and *rad53* mutants.

We used a red-white sectoring assay to identify nonsectoring *rod* (*RAD53* overproduction dependent) mutants (*11*, *12*), which depended for survival on a color-marked plasmid that overexpressed *RAD53*. These mutants failed to survive plasmid loss (Fig. 1A) and displayed checkpoint-defective phenotypes when replication was blocked by hydroxyurea (HU). One *rod* mutant was allelic to *MEC1* (*3*), as determined by complementation and linkage, and was named *mec1-22*. *MEC1* on a centromeric plasmid restored wild-type HU resistance to *mec1-22* and relieved its dependence on overproduction of *RAD53* (Fig. 1B).

To determine the extent of the suppression of *mec1* mutants, we examined the ability of *RAD53* to suppress additional *mec1* phenotypes. *RAD53* overproduction suppressed the HU sensitivity of *mec1-21* (Fig. 2A) and of *mec1-1* (*13*) and the lethality of a *mec1* deletion (Fig. 2B), which indicates that such overproduction can provide the essential function of *MEC1*. It did not restore HU resistance to levels found in the wild type, which indicates that it cannot restore full checkpoint function (*13*). *DUN1* overproduction suppresses a null allele of YBR1022 (*MEC1*) (*14*). We confirmed this in our strain background (Fig. 2B) and showed that the ability of *DUN1* to suppress depended on its kinase activity because the *dun1-2*^{K229R} catalytically defective mutant did not suppress (Fig. 2B). This result raises the possibility that the ability of *RAD53* to suppress *mec1* mutants might be through an effect on Dun1p function.

ATM shares more sequence similarity with YBL088 (*TEL1*) than with *MEC1* but has more in common phenotypically with *mec1* mutants (*9*). To examine the function of *TEL1* in this pathway, we disrupted this gene in wild-type, *rad53*, and *mec1* mutants. The *tel1* mutations alone or in combination with *rad53* mutations had no effect on cell growth, cell cycle checkpoints, or DNA damage sensitivity relative to their respective isogenic *TEL1* parental strains (*15*, *16*). However, when combined with *mec1* mutations, *tel1* deficiency caused extremely slow growth with increased cell death per

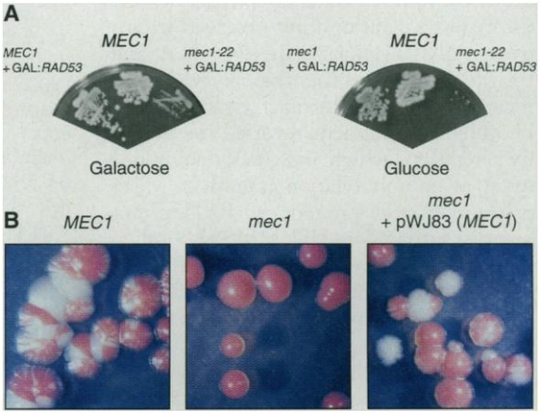

Fig. 1. Isolation of a *mec1* mutant dependent on overproduction of *RAD53*. Strains used were the following: YCH128 (*MATa, MEC1, lys2, ade2, ade3, ura3, leu2*, and *his3*); Y650 [YCH128 containing pWJ28 (*URA3 ADE3 GAL:RAD53*)]; and Y651, as Y650 but with *mec1-22*. Y650 was mutagenized, and colonies growing on galactose that failed to survive pWJ28 loss were identified by their homogeneous red color and analyzed as described (*11*, *12*). (**A**) Characterization of the galactose dependency of Y651 (*mec1-22*), a nonsectoring mutant derivative of Y650. Mec$^+$ YCH128 and Y650 strains can grow on both glucose and galactose as carbon sources. However, Y651 (*mec1-22*) can grow only on galactose, which indicates that it depends on high *RAD53* expression from the *GAL1* promoter. (**B**) Introduction of a single copy of *MEC1* into Y651(*mec1-22*) relieves the dependency on *RAD53* overproduction. Left: Parental Y650 stain (YCH128 + pWJ28) forms red colonies with white sectors, indicating pWJ28 (*GAL:RAD53*) loss . Middle: Y651 (*mec1-22*) forms homogeneously red colonies (nonsectoring), indicating that the presence of pWJ28 is essential for survival of the mutant cells. Right: Y651 containing *MEC1* on pWJ83 (*MEC1 CEN LEU2*) shows sectoring, indicating loss of pWJ28 (*GAL:RAD53*) similar to that observed for the parental Y650 strain. Plasmid pWJ83 also restores wild-type HU resistance, which demonstrates complementation of *mec1-22* by *MEC1* (*21*).

Verna and Mars McLean Department of Biochemistry, Department of Molecular and Human Genetics, Howard Hughes Medical Institute, Baylor College of Medicine, One Baylor Plaza, Houston, TX 77030, USA.

*To whom correspondence should be addressed.

generation and increased sensitivity to DNA damage and HU (Fig. 2, C and D). During the course of these studies, Morrow *et al.* (*17*) made similar observations and additionally determined that a second copy of *TEL1* can suppress a partial *mec1* deletion (*17*). These data indicate that *TEL1* shares functions with *MEC1* but does not control a separate parallel checkpoint pathway because *rad53 tel1* mutants are no more defective than *rad53* alone (Fig. 2C).

We also examined the ability of *RAD53* overproduction to suppress deficiencies in *mec1 tel1* double mutants. *RAD53* overproduction suppressed the rate of killing by HU in liquid culture of both *mec1* (*13*) and *mec1 tel1* mutants (Fig. 2E). It also suppressed the sensitivity to ultraviolet light of these mutant combinations (Fig. 2F). These data suggest that *RAD53* functions downstream of *MEC1* and *TEL1* in the DNA damage response pathway and that the essential function of *MEC1* is likely to be mediated by *RAD53*.

If *RAD53* transduces the DNA damage signal, it should respond to damage. Consistent with this hypothesis, Rad53p shows altered electrophoretic mobility in response to treatment with methyl methane sulfonate (MMS) or HU (Fig. 3A) (*18*–*20*). The identity of Rad53p was demonstrated by its specific absence in a *rad53* deletion strain that was alive because of the presence of a suppressor (Fig. 3A, lane 1) (*13*). Because these agents also partially synchronize cells in the S phase, we examined the mobility of Rad53p through the cell cycle to determine if this mobility shift resulted from synchronization. *RAD53* mRNA is regulated by the cell cycle (*3*, *4*), and Rad53p also increases during the S-G_2 phase (Fig. 3B). However, the S-G_2 form of Rad53p consists of only the fastest migrating form observed in untreated asynchronous cells (Fig. 3, A and B), which indicates that the observed modification is not an artifact of synchrony. Phosphatase treatment reversed the mobility alteration, which indicates that it is a result of phosphorylation (Fig. 3C). MMS produces a more pronounced Rad53p mobility shift than does HU. MMS also induces higher levels of *RNR3* than HU (*5*), which suggests that the degree of Rad53p phosphorylation may be correlated with the strength of signal generated by Rad53p.

To establish the genetic pathway controlling these responses, we examined Rad53p modification in checkpoint-defective mutants. Modification depended on *MEC1* but not *RAD9*. Insufficient Rad53p was detected in the *rad53-21* mutant to determine the modification dependency on *RAD53* itself. However, the HU- and MMS-induced phosphorylation of Rad53p remained intact in the checkpoint and kinase-defective *rad53-31*^{K227A} mutant strain (*21*), although the Rad53p levels did not increase as was observed with the wild-type protein. These results indicate that *RAD53* responds to DNA damage and replication blocks and is a transducer of these signals to the checkpoint apparatus and that *MEC1* acts upstream of *RAD53*, perhaps directly phosphorylating and activating Rad53p. We have also observed an increase in Rad53p autophosphorylation activity from damaged cells (*21*). These results further indicate that Rad53p kinase activity is involved in its own up-regulation in response to HU and MMS. That Rad53p is modified in asynchronous Δ*rad9* cells indicates that there are other checkpoint components or sensors—for example, *POL2*—that transduce the checkpoint signal to Rad53p in a *RAD9*-independent manner.

Because of the genetic interaction between *MEC1* and *TEL1*, we examined whether *TEL1* also regulates *RAD53*. *TEL1* on a centromeric plasmid rescues the viability of Δ*mec1* and *rad53-21* Δ*mec1* double mutants, but the double mutant is more sensitive to HU, which indicates that *TEL1* requires *RAD53* for efficient suppression of *mec1*. In addition, HU- and MMS-induced phosphorylation of Rad53p was restored in a Δ*mec1* strain with a plasmid copy of *TEL1* but not in the Δ*mec1* strain rescued by overexpression of the *DUN1* kinase (Fig. 3E).

Taken together, our results support a model (Fig. 4) in which *MEC1* and *TEL1* perform overlapping functions in response to DNA damage and replication blocks and in some way activate the *RAD53* protein kinase, perhaps by direct phosphorylation, to control the cell cycle and transcriptional responses to DNA damage. Two proteins of this lipid kinase structural family have protein kinase activity (*22*). Phosphorylation of Rad53p correlates with and may cause activation of Dun1p, which controls the transcriptional response to DNA damage. Mec1p, Rad53p, and Dun1p may be components of a kinase cascade. Presumably, *RAD53* controls additional proteins that function in cell cycle arrest.

These results may be relevant to the function of ATM and cell cycle control in mammalian cells. The ATM controls cell cycle arrest, the kinetics of p53 activation, and telomere length (*1*). *MEC1* also controls the G_1 and G_2 cell cycle arrests, and *TEL1* controls telomere lengths. Thus, the gene encoding ATM has properties characteristic of both *MEC1 and TEL1*. However, *MEC1*, like *rad3* and *mei-41*, also controls the S phase checkpoint in response to replication blocks, a property not yet demonstrated for ATM-defective mutants. This

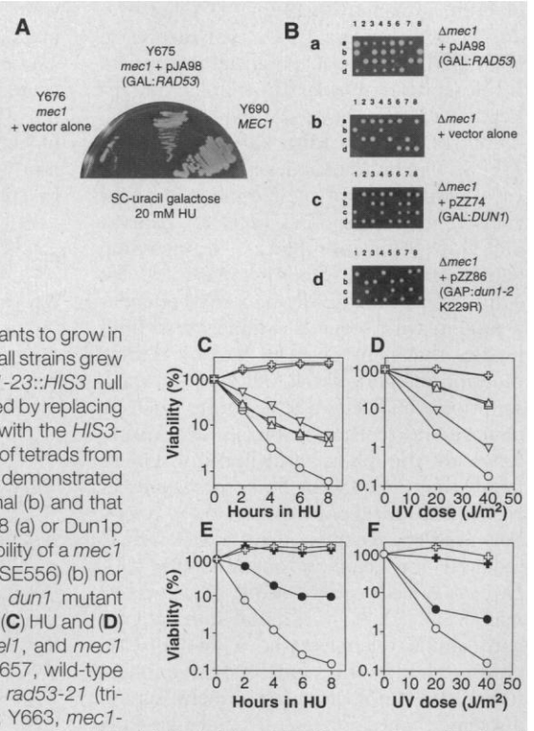

Fig. 2. Overlapping functions of *MEC1* and *TEL1* that can be suppressed by *RAD53* overproduction. (**A**) Partial suppression of the HU sensitivity of *mec1-21* Y675 in cells overexpressing *RAD53*. Y690 (*MEC1*), Y675 [*mec1-21* containing pJA98 (*URA3 GAL:RAD53*)], and Y676 [*mec1-21* + pSE556 (*URA3*)] were streaked on synthetic complete (SC)–uracil media containing galactose as a carbon source and 20 mM HU at 30°C. Y676 failed to grow in 20 mM HU at 30°C, and overexpression of *RAD53* (Y675) restored the ability of *mec1-21* mutants to grow in the presence of HU. In the absence of HU, all strains grew equally well. (**B**) Suppression of the *mec1-23*::*HIS3* null mutation. The *mec1-23* mutant was created by replacing a 6.5-kb Stu I to Afl II fragment of *MEC1* with the *HIS3-KAN* cassette from pJA51 (*26*). Dissection of tetrads from a diploid heterozygous for the disruption demonstrated that the *mec1-23*::*HIS3* mutation was lethal (b) and that the overproduction of Rad53p from pJA98 (a) or Dun1p from pZZ74 (c) suppressed the loss of viability of a *mec1* deletion. However, neither vector alone (pSE556) (b) nor the overproduction of a kinase-defective *dun1* mutant (pZZ86) (d) rescued the *mec1* null mutant. (**C**) HU and (**D**) ultraviolet light (UV) sensitivity of *mec1*, *tel1*, and *mec1 tel1* double mutants. Strains used were Y657, wild-type (crosses); Y658, Δ*tel1* (diamonds); Y659, *rad53-21* (triangles); Y660, *rad53-21* Δ*tel1* (squares); Y663, *mec1-21* (upside-down triangles); and Y664, *mec1-21* Δ*tel1* (circles). (**E** and **F**) Suppression of HU and ultraviolet light sensitivity of *mec1-21* Δ*tel1* mutants by overexpression of *RAD53* from pQL45 (*ADH:RAD53*). In (E), log phase cells were incubated with or without 0.2 M HU for the indicated times and plated onto YPD (yeast extract, peptone, and dextrose) plates to determine survival. For killing by ultraviolet light (F), cells were plated onto YPD and irradiated at the indicated doses with ultraviolet light. Strains used were Y664, *mec1-21* Δ*tel1* (open circles); Y668, *mec1-21* Δ*tel1* + pQL45 (closed circles); Y661, wild type (open crosses); and Y665, wild type + pQL45 (closed crosses) (*14*).

difference might represent a divergence in the functions of these genes or may be a result of the different ways mitosis is controlled in different organisms. A human gene belonging to the *MEC1-rad3* family has been identified; this is the *ATR* gene (*23*), which demonstrates that there are two structurally distinct families of proteins, the *ATM-TEL1* and the *ATR-rad3/MEC1* families. These families have overlapping functions in budding yeast and are likely to have such functions in mammals as well.

RAD53 is conserved in evolution. Recently, a *RAD53*-related *S. pombe* gene, *cds1* (*24*), was reported to have a role in the response to DNA replication blocks. The degree of structural and functional conservation between these distantly related species suggests the existence of a related gene in higher eukaryotes. If so, this gene may be regulated by ATM in response to DNA damage and may control p53. Such a protein would have an important role in the response to DNA damage and tumor suppression.

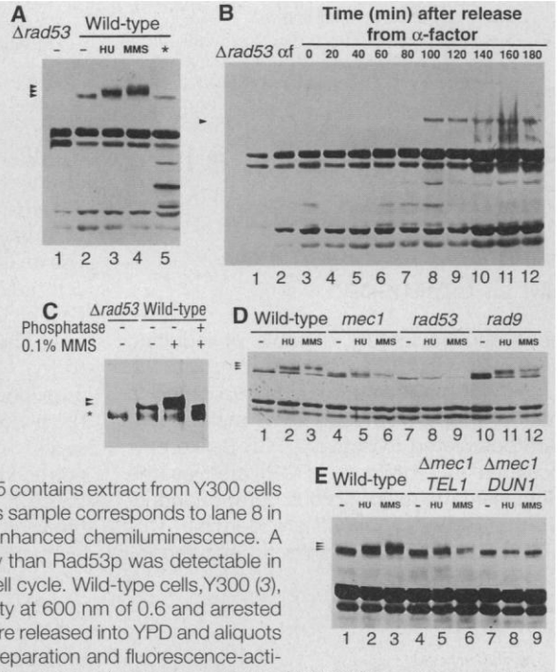

Fig. 3. Control of phosphorylation of Rad53p in response to DNA damage and replication blocks by *MEC1* and *TEL1*. Arrows refer to the different forms of Rad53p. (**A**) Wild-type cells (optical density at 600 nm = 0.6) were treated with 200 mM HU or 0.1 % MMS for 2 hours, protein extracts were prepared, separated by SDS-PAGE, and immunoblotted with antibodies to Rad53p (*18–20, 27*). Lane 1 contains extract from asynchronous culture of the *Δrad53* strain (Y677) rescued by a plasmid containing a high copy suppressor (*13*). Lanes 2 to 4 contain extracts from parallel asynchronous cultures of wild-type cells, Y300 (*3*), incubated in the absence (lane 2) or presence (lane 3) of 200 mM HU or 0.1% MMS (lane 4) for 2 hours at 30°C. Lane 5 contains extract from Y300 cells 100 min after release from α-factor; this sample corresponds to lane 8 in Fig. 3B. Proteins were detected by enhanced chemiluminescence. A faint band with a slightly faster mobility than Rad53p was detectable in the *Δrad53* strain. (**B**) Rad53p in the cell cycle. Wild-type cells,Y300 (*3*), were grown in YPD to an optical density at 600 nm of 0.6 and arrested with α-factor as described (*3*). Cells were released into YPD and aliquots taken at 20-min intervals for protein preparation and fluorescence-activated cell sorting analysis. Proteins (150 μg per lane) were separated by SDS-PAGE and immunoblotted with antibodies to Rad53p as in (A). The 100-min time point was used in (A) to compare the mobility of the S-G_2 form of Rad53p to that observed in response to DNA damage and replication blocks (A). Lane 1, *Δrad53* control extracts; lane 2, extracts from α-factor–arrested cells; lanes 3 to 11 contain extracts prepared at the indicated times after release from α-factor. (**C**) Phosphorylation of Rad53p in response to DNA damage. Wild-type cells, Y300 (*3*), were grown in the presence or absence of 0.1% MMS, and protein was prepared. Rad53p was immunoprecipitated from wild-type and *Δrad53* extracts (1 mg per lane) with antibodies to Rad53p (*18*). An immunoprecipitate from an MMS-treated sample was treated with 10 units of calf intestinal phosphatase (New England Biolabs) at 37°C for 25 min., separated by SDS-PAGE, and immunoblotted with the use of antibodies to Rad53p as in (A). The asterisk indicates a cross-reactive protein found in the *Δrad53* null mutant. (**D**) Regulation of Rad53p in checkpoint-defective mutants. Strains used were TWY397 (wild-type); TWY308 (*mec1-1*); TWY312 [*mec2-1* (*rad53*)]; and TWY398 (*Δrad9::LEU2*). Strains were treated as in (A), and Rad53p was visualized by immunoblotting. (**E**) *TEL1* can restore regulated phosphorylation to Rad53p in the *Δmec1* strain. pDM197 (*CEN TEL1*) (*17*) or pZZ74 (*GAP:DUN1*) (*5*) was introduced into the *MEC1/mec1-23::HIS3* diploid and sporulated. Tetrad dissection demonstrated that either plasmid can suppress *Δmec1* (*21*). Haploid wild-type (lanes 1 through 3) and *Δmec1* strains containing either pDM197 (lanes 4 through 6) or pZZ74 (lanes 7 through 9) were treated with HU, MMS, or neither, as in (A). The strains used in lanes 4 through 9 have either *TEL1* or *DUN1* overproduced.

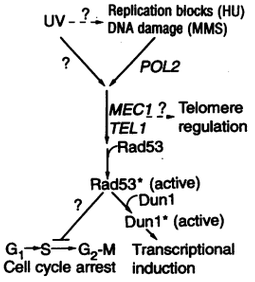

Fig. 4. A model describing the DNA damage signal transduction pathway in yeast. In the G_1 or G_2-M phases, DNA damage (from ultraviolet light) generates a signal that is sensed by an unknown sensor that activates cell cycle arrest in a *RAD9*-dependent manner. During the S phase, DNA damage (MMS), nucleotide depletion (HU), or mutational inactivation of DNA polymerases blocks DNA replication, which is subsequently sensed by *POL2* (Pol ε). The checkpoint activation signal generated by *POL2* and other sensors is transduced through the *MEC1* and *TEL1* kinases, leading to phosphorylation of Rad53p, which is denoted by the asterisk (Rad53*). Whether *MEC1* and *TEL1* are actually transducing the signal or are merely necessary for its transduction awaits elucidation of their biochemical activities. Rad53* then causes cell cycle arrest and the activation of the Dun1 kinase, Dun1*, to induce the expression of damage-inducible genes. *POL2* is proposed to be at the head of the pathway above *MEC1*, *TEL1*, and *RAD53* on the basis of its genetic and biochemical properties.

REFERENCES AND NOTES

1. L. S. Cox and D. P. Lane, *Bioessays* **17**, 501 (1995); E. C. Friedberg, G. C. Walker, W. Siede, *DNA Repair and Mutagenesis* (American Society for Microbiology Press, Washington, DC, 1995), pp. 662–668.
2. T. A. Navas, Z. Zhou, S. J. Elledge, *Cell* **80**, 29 (1995).
3. T. A. Weinert, G. L. Kiser, L. H. Hartwell, *Genes Dev.* **8**, 652 (1994); R. Kato and H. Ogawa, *Nucleic Acids Res.* **22**, 3104 (1994); J. B. Allen *et al.*, *Genes Dev.* **8**, 2416 (1994). *MEC1/SAD3/ESR1* and *SAD1/RAD53/MEC2/SPK1* have been isolated and named several times; for the sake of brevity, we will use names corresponding to the first description in the literature, *MEC1* and *RAD53* (*25*). In this regard, our original *sad1-1* allele has been renamed *rad53-21*, and our original *sad3-1* allele is called *mec1-21*.
4. P. Zheng *et al.*, *Mol. Cell. Biol.* **13**, 5829 (1993); D. F. Stern, P. Zheng, D. R. Beidler, C. Zerillo, *ibid.* **11**, 987 (1991).
5. Z. Zhou and S. J. Elledge, *Cell* **75**, 1119 (1993).
6. A. Nasim and M. A. Hannan, *Can. J. Genet. Cytol.* **19**, 323 (1977); B. L. Seaton, J. Yucel, P. Sunnerhagen, S. Subramani, *Gene* **119**, 83 (1992); T. Enoch, A. M. Carr, P. Nurse, *Genes Dev.* **6**, 2035 (1992).
7. A. J. Lustig and T. D. Petes, *Proc. Natl. Acad. Sci. U.S.A.* **83**, 1398 (1986).
8. K. L. Hari *et al.*, *Cell* **82**, 815 (1995).
9. Y. Shiloh, *Eur. J. Hum. Genet.* **3**, 116 (1995); K. Savitsky *et al.*, *Science* **268**, 1749 (1995); K. Savitsky *et al.*, *Hum. Mol. Genet.* **4**, 2025 (1995).
10. M. Swift, P. J. Reitnauer, D. Morrell, C. Chase, *N. Engl. J. Med.* **316**, 1289 (1987); M. Swift, D. Morrell, C. Chase, *ibid.* **325**, 1831 (1991).
11. pWJ28 contains *RAD53* under control of *GAL1* on pMW29 (*CEN URA ADE3*).
12. J. E. Kranz and C. Holm, *Proc. Natl. Acad. Sci. U.S.A.* **87**, 6629 (1990); H. A. Zieler, M. Walberg, P. Berg, *Mol. Cell Biol.* **15**, 3227 (1995).
13. B. A. Desany and S. J. Elledge, unpublished results.
14. F. Nasr *et al.*, *C. R. Acad. Sci. III* **317**, 607 (1994).
15. All strains are isogenic to Y323. The *Δtel1* allele was made by replacement (*16*) of one copy of the entire *TEL1* open reading frame in the diploid Y323 with *HIS3*, creating Y653. The replacement construct was made by recombinant polymerase chain reaction (PCR) using the splicing by the overlap extension (SOEing) method (*16*), bringing together three PCR products generated with the following pairs of primers: tggtgtcatcgctaatc, atgctagggaacaggaccgtgcagcaaaatatgcatattgtacggc, accagccgtacaatatgcatattttgctgcacggtcctg, tcatcacattgagtttgtacattaccagaatgacacg, tatagaatga, taatagtgaagatccgcag, and gcatcattctatacgtgtcattctggtaatgtacaaactcaatgtgatg. Y654 (*Δtel1*) was isolated by sporulation of Y653. The haploid strains used in Fig. 2, C through F, were derived from crosses between Y654 and Trp^+ derivatives of Y301 (*rad53-21*) or Y306 (*mec1-21*) (*3*) called Y655 and Y656 and are all isogenic to each other. Plasmid pQL45 was introduced into wild-type and *mec1-21 Δtel1* strains derived from the cross of Y653 and Y656 to make Y665 and Y668. Plasmid pQL45 places *RAD53* under control of the *ADH* promoter on a *URA3 CEN* vector.
16. R. Rothstein, *Methods Enzymol.* **194**, 281 (1991); R. M. Horton *et al.*, *Gene* **77**, 61 (1989); R. D. Gietz and R. A. Woods, in *Molecular Genetics of Yeast: A Practical Approach*, J. R. Johnston, Ed. (Oxford Univ. Press, New York, 1994), chap. 8.

17. D. M. Morrow, D. Tagle, Y. Shiloh, F. Collins, P. Hieter, *Cell* **82**, 831 (1995).
18. Affinity-purified Rad53p antibody was prepared from glutathione-S-transferase–Rad53 as described (*19*). For immunoblot analysis, 150 μg of cell extracts was run on 8% SDS–polyacrylamide gel electrophoresis (SDS-PAGE), transferred to polyvinylidene difluoride (PVDF) (Dupont) membrane as described (*19*), and visualized by enhanced chemiluminescence (Amersham). For immunoprecipitations, 1 mg of protein extract was incubated with Rad53p affinity-purified antibody in 25 mM Hepes (pH 7.6), 0.1 M NaCl, 5 mM $MgCl_2$, 0.1 mM EDTA, 1 mM phenylmethylsulfonyl fluoride, 200 μg/ml of bovine serum albumin, 0.1% Tween-20, 0.1 mM benzamidine, 1 μM aprotinin, 0.1 μg/ml each of leupeptin, soybean trypsin inhibitor, pepstatin, and antipain, 0.1 mM Na_3VO_4, and 30 mM NaF for 1 hour at 4°C. Protein-antibody complexes were precipitated with protein Sepharose A and washed with 25 mM Hepes (pH 7.6), 1% (w/v) Triton X-100, 10% (v/v) glycerol, 1 μM aprotinin, 0.5 M NaCl, 0.1 mM Na_3VO_4, and 30 mM NaF.
19. E. Harlow and D. Lane, *Antibodies: A Laboratory Manual* (Cold Spring Harbor Laboratory Press, Cold Spring Harbor, NY, 1988).
20. S. J. Elledge and R. W. Davis, *Mol. Cell. Biol.* **7**, 2783 (1987).
21. Y. Sanchez *et al.*, data not shown.
22. J. H. Stack and S. D. Emr, *J. Biol. Chem.* **269**, 31552 (1994); R. Dhand *et al.*, *EMBO J.* **13**, 522 (1994).
23. N. Bentley and A. Carr, personal communication.
24. H. Murakami and H. Okayama, *Nature* **374**, 817 (1995).
25. C. W. Moore, *Mutat. Res.* **51**, 165 (1978).
26. J. B. Allen and S. J. Elledge, *Yeast* **10**, 1267 (1994).
27. H. Towbin, T. Staehelin, J. Gordon, *Proc. Natl. Acad. Sci. U.S.A.* **76**, 4350 (1979).
28. We thank T. Weinert, C. Hardy, D. Morrow, P. Hieter, R. Richman, and M. Walberg for reagents and D. Achille and W. Schober for technical assistance. Supported by NIH training grant DK07696 to Y.S. and NIH grant GM44664 and Welch grant Q1186 to S.J.E. S.J.E. is a Pew Scholar in the Biomedical Sciences and an Investigator of the Howard Hughes Medical Institute.

8 September 1995; accepted 4 December 1995

Bone Morphogenetic Protein–1: The Type I Procollagen C–Proteinase

Efrat Kessler, Kazuhiko Takahara, Luba Biniaminov, Marina Brusel, Daniel S. Greenspan

Bone morphogenetic proteins (BMPs) are bone-derived factors capable of inducing ectopic bone formation. Unlike other BMPs, BMP-1 is not like transforming growth factor–β (TGF-β), but it is the prototype of a family of putative proteases implicated in pattern formation during development in diverse organisms. Although some members of this group, such as *Drosophila* tolloid (TLD), are postulated to activate TGF-β–like proteins, actual substrates are unknown. Procollagen C–proteinase (PCP) cleaves the COOH-propeptides of procollagens I, II, and III to yield the major fibrous components of vertebrate extracellular matrix. Here it is shown that BMP-1 and PCP are identical. This demonstration of enzymatic activity for a BMP-1/TLD-like protein links an enzyme involved in matrix deposition to genes involved in pattern formation.

After the isolation of BMP-1 peptides from osteogenetic fractions of bone (*1*), proteins involved in morphogenetic patterning, such as *Drosophila* TLD and TLR-1 (*2–4*) and sea urchin BP10 and SpAN (*5*), were isolated and found to be structural homologs of BMP-1. Each contains an NH_2-terminal astacin-like metalloprotease domain (*6*) followed by varying numbers of epidermal growth factor (EGF) motifs and CUB protein-protein interaction domains (*7*). Substrates have not been demonstrated for any member of this family of putative proteases. Although évidence suggests they may function in morphogenesis by activating TGF-β–like molecules (*1*, *8*), it has also been suggested that BMP-1/TLD-like proteases may modify matrix components, thus influencing cell fate decisions by altering cell-matrix interactions (*3*).

Collagen types I, II, and III are the major fibrous components of vertebrate matrix, and their orderly deposition is critical for normal morphogenesis. They are synthesized as procollagens, precursors with NH_2- and COOH-terminal propeptides that must be cleaved to yield mature monomers capable of forming fibrils (*9*). PCP, the physiological activity that cleaves procollagen I, II, and III COOH-propeptides, shares a number of features with BMP-1. It is a secreted N-glycosylated metalloprotease that requires calcium for optimal activity (*10–12*), and it is crucial for cartilage and bone formation, because collagen types II and I, respectively, are the major protein constituents of these tissues. Similarly, BMP-1 is implicated in de novo endochondral bone formation (*1*) and is also a metalloprotease with multiple sites for potential N-linked glycosylation and EGF-like sequences that may confer calcium dependence (*13*) on binding activities of adjacent CUB domains. The molecular mass of mammalian PCP (*11*) is close to that expected for mature BMP-1 (*1*). PCP activity is stimulated by the procollagen C–proteinase enhancer (PCPE), a glycoprotein that binds the type I procollagen COOH-propeptide by means of CUB domains (*11*, *14*). Because PCP also binds the COOH-propeptide (*11*, *12*) and PCPE itself (*15*), we noted that PCP may contain CUB domains and, thus, be BMP-1–like (*14*).

To investigate possible correlations between BMP-1 and PCP, we compared the properties of secreted recombinant BMP-1 (rBMP-1) produced by a baculovirus system (*16*) with those of purified mouse PCP (*17*). We first examined whether rBMP-1 has PCP-like activity (*17*). Type I procollagen was incubated with conditioned media from cells infected with baculovirus containing a BMP-1 complementary DNA (cDNA) insert. The type I procollagen was processed to yield the disulfide-linked COOH-propeptide and pNα1 and pNα2 chains as the major products (Fig. 1A) (*18*). No nonspecific cleavages were evident. The SDS–polyacrylamide gel electrophoresis (SDS-PAGE) mobilities of rBMP-1–generated products were identical to those of products generated by mouse PCP. Cleavages did not occur when procollagen was incubated with conditioned media from cells infected with wild-type virus (Fig. 1, A and B) or from uninfected cells (*19*). Electrophoretic mobilities of reduced propeptide subunits C1 and C2 from human (Fig. 1B) or chick (Fig. 1C) type I procollagen were also indistinguishable when released by rBMP-1 or PCP.

These results were consistent with the

Table 1. Inhibition profiles of rBMP-1 and procollagen C–proteinase (PCP). DFP, diisopropyl fluorophosphate; PMSF, phenylmethylsulfonyl fluoride; SBTI, soybean trypsin inhibitor. ND, not done.

Inhibitor	Concentration (mM)	Inhibition (%) with	
		rBMP-1*	PCP†
EDTA	10	100	100
EGTA	10	100	100
1,10-phenanthroline	1	100	98
1,7-phenanthroline	1	0	ND
1,4-phenanthroline	1	89	ND
L-Lysine	10	89	80
L-Arginine	10	92	86
ε-Amino caproic acid	10	81	80
Dithiothreitol	1	100	100
DFP	1	10	11‡
PMSF	0.4	0	13
SBTI	10§	0	10
Leupeptin	10§	0	0

*rBMP-1 activity was determined with the assay for PCP activity described in Kessler *et al.* (*12*). †PCP data are from Kessler *et al.* (*12*). ‡Value for inhibition of PCP by DFP is from Hojima *et al.* (*10*). §10 μg/ml.

E. Kessler, L. Biniaminov, M. Brusel, Maurice and Gabriela Goldschleger Eye Research Institute, Tel Aviv University Sackler Faculty of Medicine, Sheba Medical Center, Tel Hashomer, 52621 Israel.
K. Takahara and D. S. Greenspan, Department of Pathology and Laboratory Medicine, University of Wisconsin, Madison, WI 53706, USA.